Journal of Applied Fluid Mechanics, Vol. 11, No. 4, pp. 1089-1100, 2018.
Available online at www.jafmonline.net, ISSN 1735-3572, EISSN 1735-3645.
DOI: 10.29252/jafm.11.04.27699

A Performance Analysis on Pressure Loss and Airflow Diffusion in a Chamber with Perforated V-Profile Diffuser Designed for Air Handling Units (AHUs)

M. S. Kamer[1], A. Erdogan[2], E. Tacgun[2], K. Sonmez[1], A. Kaya[1], I. G. Aksoy[2†] and S. Canbazoglu[2]

[1] *Department of Mechanical Engineering, Faculty of Engineering and Architecture, Kahramanmaras Sutcu Imam University, 46100 Kahramanmaras, Turkey*
[2] *Department of Mechanical Engineering, Faculty of Engineering, Inonu University, 44280 Malatya, Turkey*

†*Corresponding Author Email: gaksoy@inonu.edu.tr*

(Received February 17, 2017; accepted March 7, 2018)

ABSTRACT

Outlet cross-sectional area of fans used in air handling units is smaller than cross-sectional area of chambers which are located next to the fan. In order to ensure efficiently operating of the air handling units, it is required that the air flows through a perforated diffuser to create a uniform air diffusion from fan outlet to following chamber with a minimum pressure loss and uniform velocity distribution. In this concept, numerical simulations and experiments were performed for the chamber with perforated V-profile diffuser, which is often used in air handling units because of its simple geometry and easy manufacturing. Pressure losses were firstly obtained experimentally for different air velocities in the chamber. Then a performance analysis on the air flow diffusion and pressure losses inside chamber with perforated V-profile diffuser for different geometric parameters such as entry length, apex angle, geometry and pattern of hole, plate thickness, porosity and surface roughness has been carried out numerically. It is seen that the experimental results validated with the numerical turbulence model results.

Keywords: Computational fluid dynamics (CFD); Pressure loss; Air handling units (AHUs); Perforated diffuser; Fan.

NOMENCLATURE

$C_{1\varepsilon}, C_{2\varepsilon}$	constants of standard $k-\varepsilon$ turbulent model
C_μ	constant
D_h	hydraulic diameter
G_k	turbulent kinetic energy production
k	turbulent kinetic energy
L	length of entry section of the air to the chamber
P	static pressure
R	roughness
Re	Reynolds number
t	thickness
u	horizontal (x) velocity component
α	apex angle of diffuser
δ	porosity
ε	dissipation ratio
μ	dynamic viscosity
μ_t	turbulent viscosity
ν	kinematic viscosity
ρ	fluid density
σ_ε	turbulent Prandtl number for ε
σ_k	turbulent Prandtl number for k

1. INTRODUCTION

Average air velocities at discharge section of suction and/or supply fan is in the order of 8-15 m/s and airflow velocity distribution is much different from that of the fully-developed turbulent flow (SMACNA 2006). Air exiting from the fan contacts with a certain portion of the chamber surface of HVAC equipment such as heating/cooling coils, silencer (sound attenuator), filter or heat recovery elements which are located after the fan if there is not any sufficient chamber length. Therefore, a chamber having a length approximately 3.5-3.7 times of the fan impeller diameter (Fig. 1a) or a

shorter chamber including a perforated diffuser must be used (Fig. 1b).

The chambers with perforated diffuser having the length of approximately 0.8-1.5 times of the fan impeller diameter facilitate the air diffusion to keep the working efficiency of the chambers such as heating/cooling coils, silencer, mixing and filter or heat recovery element at the desired level (Bilge 2010). When a chamber with perforated diffuser is used in the air handling unit (AHU), it is possible to increase the working efficiency of the chambers by a uniformly distributed airflow passing through the entire surface and consequently decreasing of total pressure losses inside the AHU is possible (Bulut *et al* 2011, Tanyol 2012).

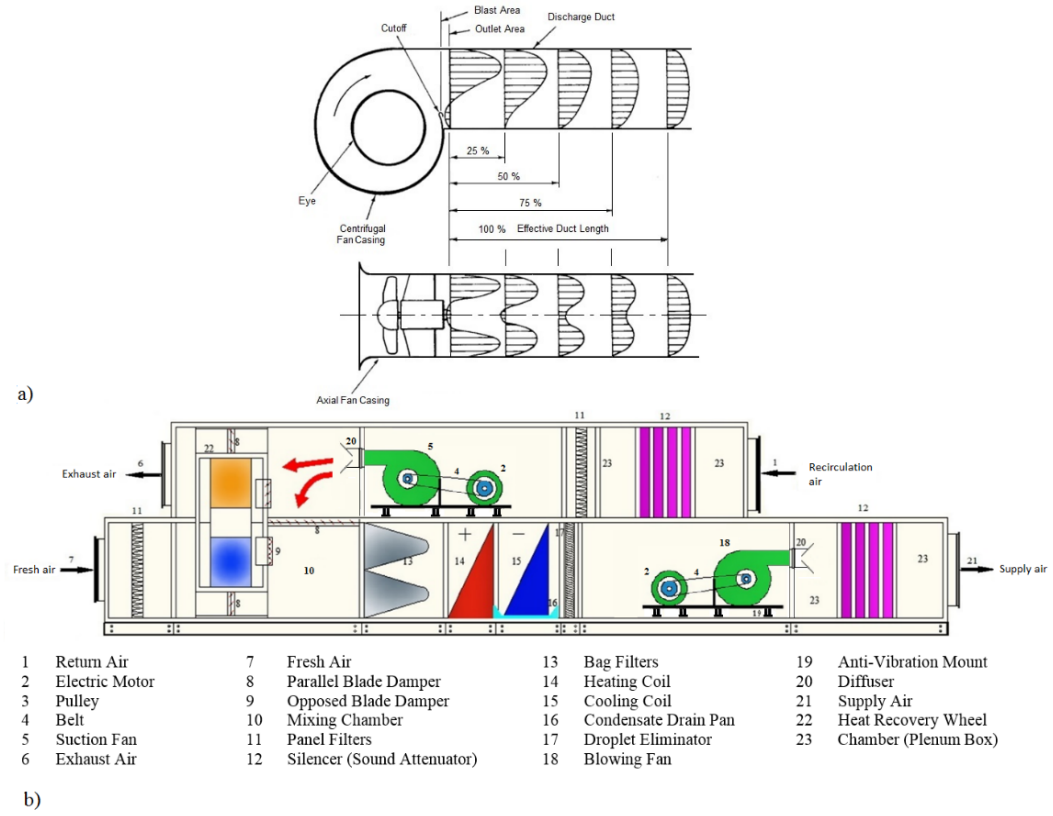

Fig. 1. a) Flow development in duct at the fan outlet, velocity profiles and effective duct length. b) An AHU arrangement with double floor including perforated diffusers after fans and before mixing chamber, rotary heat exchanger and silencer (sound attenuator).

According to market survey carried out among AHU manufacturers, it is determined that perforated diffusers cannot sufficiently ensure the expected flow performance because there is not sufficient data on flow structure in chambers with perforated diffuser. According to literature review, it was seen that only one preview CFD (computational fluid dynamics) study for a chamber with perforated diffuser in the form of truncated square pyramid was carried out and velocities at chamber exit was investigated. This numerical study is not a comprehensive scientific research on this diffuser (Bulut *et al* 2011, Tanyol 2012). Decreasing of internal pressure losses in AHU and airflow diffusion homogenously to the chambers after fan is very important. Energy efficiency in AHUs is very important and it is seen that the ratio of electric energy operation costs of fans to their life cycle cost is at the order of 40-50 % approximately (Bulut *et al* 2011, Tanyol 2012). Therefore, even small reduction in internal pressure losses in AHUs is very important. Airflow in diffuser having no perforation at a fan exit section of an AHU was investigated numerically by (Bayramgil *et al* 1998). They measured static pressure distributions on surface for different diffuser angle and showed that flow at diffuser exit was not uniform and turbulence level considerably varied with position from point to point. Some studies to determine flow characteristics for the uses of perforated plates located vertically to flow direction in wide-angle diffuser used widely electrostatic precipitator applications were carried out (Sahin 1989, Sahin *et al* 1995, Sahin and Ward-Smith 1987, Sahin and Ward-Smith 1993, Sahin and Ward-Smith 1991, Sahin and Ward-Smith 1990). However, the geometries of diffusers used in these studies are very different from those of perforated V-profile diffusers subjected to this study. Gas flow through a hole of perforated plate located vertically to flow direction were investigated by CFD the effects on the flow form and pressure loss of parameters such as Reynolds number, open porosity, hole diameter, plate thickness, surface roughness and incline angle of plate (Guo *et al* 2013). A study to obtain constant flow at the end of diffuser using perforated plate located vertically to flow direction in an asymmetric wide-angle diffuser was carried out (Noi-Mehidi *et*

al 2005). They defined that flow can be enhanced much and more and an asymmetric wide-angle diffuser can be much more user-friendly for flow control by using of perforated plates having appropriate number and location at the exit of diffuser. Determination of pressure loss coefficient for perforated plates by CFD and the obtained results were compared with experimental results (Gan and Riffat 1997). They also investigated the effect on pressure coefficient of plate thickness. The effects of plate geometry and flow regimes on pressure losses in perforated plates located vertically to flow direction in an air duct were numerically and experimentally examined (Bayazit *et al* 2014). The numerical simulation required the solution of a three dimensional, steady fluid flow. The laminar portion of the simulations has based on the full Navier-Stokes equations, while the basis of the turbulent-flow simulations has the RANS equations supplemented by a turbulence model. For the laminar flow regime, it was observed that higher pressure drops were associated with thicker plates and with the staggered-array hole pattern; higher porosities led to lower pressure drops. For the turbulent case, it was seen that the thinner plate caused higher pressure drops as did the square-array hole pattern; also, the pressure drop was found to depend on the square of the Reynolds number, indicating the dominance of momentum-based losses. Pressure loss through a variety of perforated plates having different geometrical aspects in a mean flow Reynolds number range of $2500 \le \mathrm{Re}_m \le 9500$ and a porosity range of $0.064 \le \delta \le 0.331$ for different numbers of holes ranging in $5 \le n_h \le 26$ was researched (Ozahi 2015). An expression, $Eu = 0.67\delta^{-2.24}$ describing the relationship between the pressure loss coefficient and the porosity of perforated plate has been proposed with a mean deviation of 12% for easy estimation of pressure loss coefficient at moderate Reynolds numbers of turbulent flow regime as a practical solution. Perforated plates are widely used in order to reduce flow non-uniformities, to retard on set of turbulence and to attenuate cavitation. Perforated plates are generally used for control of efficiency of any pressurized systems. Besides this, they are usually placed upstream of measurement stations in order to remove swirl effect of flow, to reduce flow non-uniformities or to create uniform flow supply air outlets (Malavasi *et al* 2012, Tullis 1989, Di Santo *et al* 1993). There are a number of heat transfer applications where homogeneous fluid flows are strictly necessary. For example, in flow passages marked by rapid enlargements in which there are duct burners, the efficiency of the combustion process critically depends on the nature of the oncoming flow (Bayazit *et al* 2014). Airflow in a AHU used in air conditioning systems was numerically investigated by using ANSYS-Fluent software to increase efficiency of a AHU (Bulut *et al* 2011). Regions caused high pressure losses by breaking flow structure were found by analysing flows in various chambers in AHU and they showed that an AHU will be able to design with an energy efficiency of 7%. The prediction of comfort properties and the numerical simulation of airflow of a computer room of a research centre were determined numerically by Ansys-Fluent Software (Abanto *et al* 2004). A four-way diffuser was used for ventilation of computer room and numerical analyses were carried out using mass flow rate as an inlet boundary condition.

As seen from literature review, flow structure in the chambers with perforated V-profile diffuser used AHUs has not been investigated. Any scientific study related with flow structure in a chamber having perforated diffuser geometry of V-profile shaped, which is often used in AHU applications because it has a simple geometric structure and easily manufacturing, has not been found. In this study, appropriate perforated V-profile diffuser geometry minimizing pressure loss and creating an uniform airflow diffusion from fan to following chambers of HVAC equipment such as heating/cooling coils, silencer (sound attenuator), filter or heat recovery elements which ensures efficiently operating of these air handling units will be determined. Pressure losses and airflow diffusion from fan outlet to following chamber will be obtained by carried out the flow analysis on the perforated V-profile diffusers having holes with cross sectional area such as circular, square and equilateral triangle. After appropriate hole geometry according to pressure loss determines, the effects on velocity distribution and pressure loss of different parameters such as apex angles, plate porosity, dimensionless entry length of diffuser, surface roughness, average airflow velocity, Reynolds number, array of hole pattern and plate thickness of diffuser have determined on perforated V-profile diffuser model will also be investigated.

2. METHODOLOGY

Using CFD analysis, a performance analysis on pressure loss and airflow diffusion in a chamber with perforated V-profile diffuser designed for AHUs have been carried out by Ansys-Fluent 14.5 software. Total eight variable parameters such as average airflow velocity, Reynolds number, thickness, porosity and apex angle of perforated plate, dimensionless entry length of diffuser, surface roughness, hole geometry and array of hole pattern were studied to determine their effects on pressure loss in chamber with perforated V-profile diffuser, velocity distribution away from the downstream edge of diffuser.

2.1 Chamber with Perforated V-Profile Diffuser

3-Dimensional CAD (Computer Aided Design) models of the chamber with perforated V-profile diffuser used in numerical simulations have been designed in SolidWorks software as shown in Fig. 2a. Cross sectional area and length of chamber with perforated V-profile diffuser are 1200 mm x 1200 mm and 600 mm, respectively. Cross sectional area (a x b) and length (L) of entry section of air to the chamber are 600 mm x 600 mm and 300 mm, respectively and it is located in the centre of

chamber. Projected exit cross sectional area of perforated V-profile diffuser are 700 mm x 700 mm and it is also located in the centre of chamber. Three type holes having circular of Ø20 mm, square of □ 18 mm and equilateral triangle of Δ 27 mm were used on the diffusers and they were located in square or staggered-array pattern. Geometrical details of diffuser and chamber with perforated V-profile diffuser were given in Figs. 2b and 2c, where α shows apex angle of diffuser.

2.2 Variable Parameters

Variable parameters considered in this study are given in Table 1. V is the average airflow velocity at cross-sectional area of fan exit, the Reynolds number (Re) is defined based on hydraulic diameter of fan exit section. x/D_h is dimensionless entry length of the diffuser, where x is the distance from fan to the diffuser. α, t, δ and R state the apex angle of diffuser, plate thickness of diffuser, plate porosity and surface roughness, respectively. Porosity or perforation ratio (δ) is defined as the ratio of total hole area on plate to total surface area with no hole.

2.3 Experimental Study

Schematic diagram of experimental setup with perforated V-profile diffuser was shown in Fig. 3. Different average airflow velocities can be obtained using a fan with frequency inverter. Point 1 and 2 in Fig. 3 shows time averaged static pressure measuring points on entry and exit section of the chamber, respectively. Cross-sectional averaged velocity measurements were carried out at the exit section of the chamber including point 2 as shown in Fig. 3. Schematic top view of static pressure

Table 1 Variable parameters

Parameters	Units	Levels					
V	m/s	9.2		10.9		11.4	
Re	-	347000		411000		430000	
x/D_h	-	0.006		0.0012		0.0018	
δ	-	0.26		0.35		0.55	
Hole geometry	-	circle		square		equilateral triangle	
Hole array pattern	-	square array			staggered array		
α	°	60	80	100	120	140	150
t	mm	1.0	2.0	2.5	3.0	4.0	5.0	6.0
R	mm	0.0003	0.008	0.0016	0.0032		

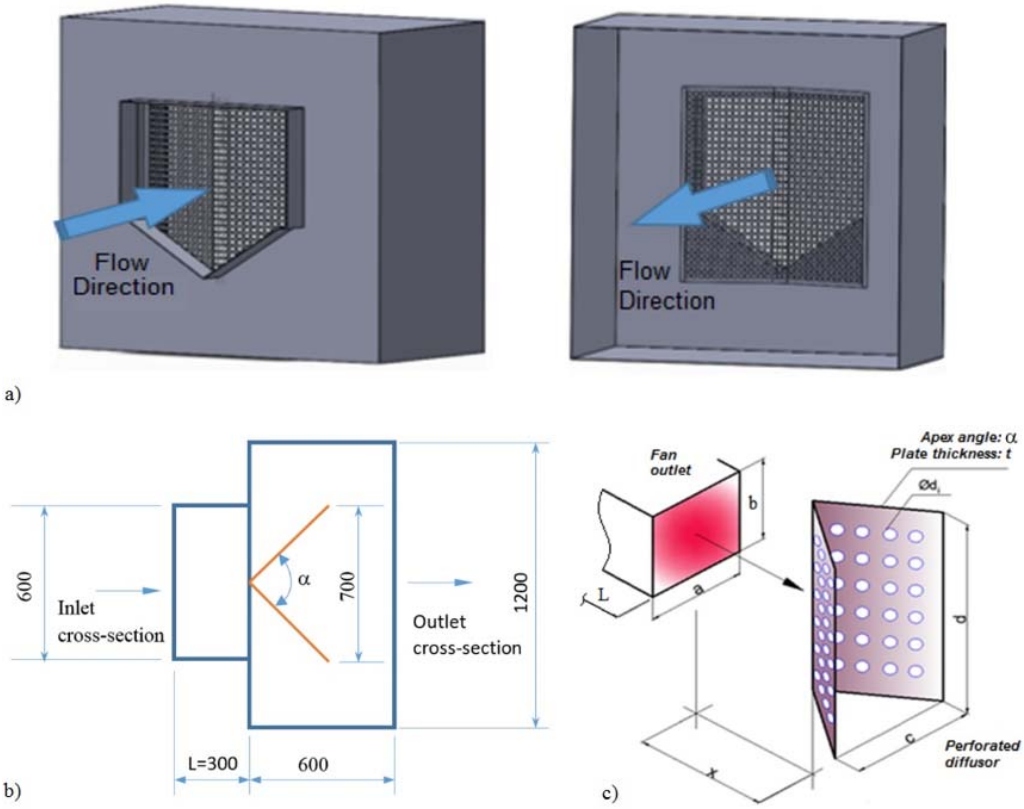

Fig. 2. a) Chamber with perforated V-profile diffuser. b) Plan view of geometrical details of chamber with perforated V-profile diffuser. c) Geometrical details of diffuser.

measuring points for chamber with perforated V-profile diffuser was also given in Fig. 4. Cross-sectional averaged values for velocity and time-averaged values for static pressure had been determined in experimental measurements. Static pressures were measured by using of flexible plastic tubes connecting between measuring instrument and static pressure holes opened appropriately on chamber. TESTO 435-4 Multifunction Instrument (static pressure and velocity measurement equipment) having static pressure and static pressure difference measurement resolution of 10 Pa and 1 Pa respectively was used for static pressures, static pressure differences and axial averaged airflow velocities (Tacgun 2016). A vane anemometer probe having ϕ=60 mm vane, 0.25-20 m/s velocity range and ∓(0.1 m/s + 1.5 % of mv) measurement accuracy is used in axial airflow velocity measurements. The mean value of relative errors in the experiments for the static pressures, static pressure differences and axial averaged airflow velocities (or Reynolds number) at fan outlet were predicted approximately as ∓1.4%, ∓0.8% and ∓1.0%, respectively. The mean value of uncertainties for the static pressures, static pressure differences and axial averaged airflow velocities (or Reynolds number) at fan outlet are estimated approximately as ∓3.0%, ∓2.0% and ∓2.0%, respectively. Experimental tests are performed by using V-profile perforated diffuser having 2 mm plate thickness, 150º apex angle and □ 20 mm square holes which are located in square-array pattern.

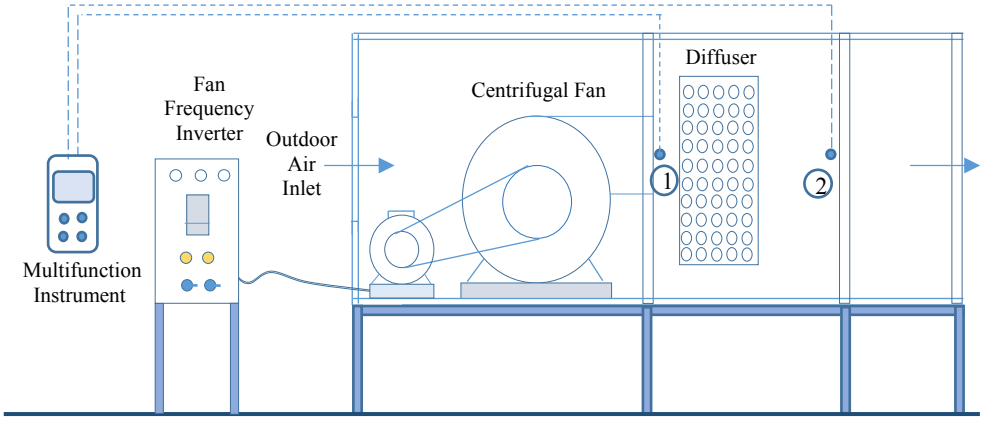

Fig. 3. Schematic diagram of experimental setup

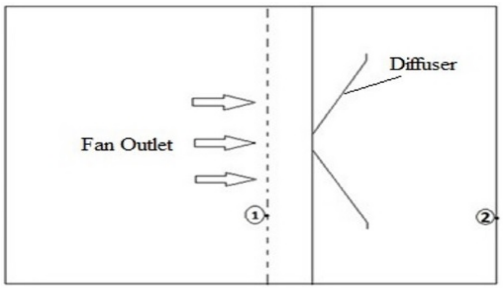

Fig. 4. Schematic plan of top view of static pressure measuring points for chamber with perforated V-profile diffuser.

2.4 Numerical Modelling

Flow analyses of selected geometries have been carried out using commercial CFD software Ansys-Fluent version 14.5. Boundary conditions were selected as 'velocity-inlet' for entry of air to the chamber with a cross section of 600 mm × 600 mm, 'pressure-outlet' for exit of air from the chamber with a cross section of 1200 mm × 1200 mm. Boundary conditions for the all other surfaces were accepted as 'stationary wall" with no-slip condition. 'Pressure-outlet' boundary condition was taken as static pressure of 700 Pa and surface roughness for surfaces defined in 'stationary wall' boundary condition taken 0.0032 mm.

Standard k-ε turbulent model, steady fluid flow and mesh dimension of 0.013 m were selected. Mesh structure produced in Ansys-Fluent Software was given in Fig. 5. Data obtained from experimental study was also used in CFD analyses. After the results obtained from experimental and numerical studies had been compared with each other, optimal solution conditions were determined by analysing different turbulent models and mesh dimensions.

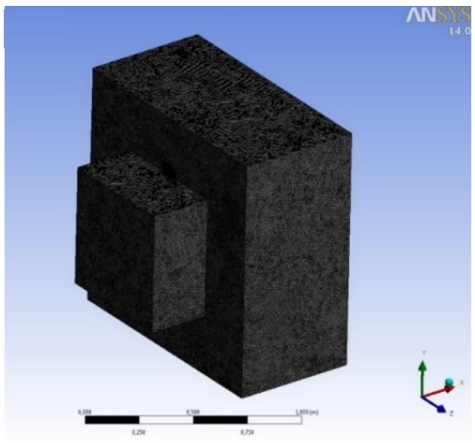

Fig. 5. Mesh structure produced for solution volume in Ansys-Fluent Software.

2.4.1 Governing Equations

Unsteady motion in a turbulent flow of an

incompressible fluid is governed by Navier-Stokes equations. The governing equations can be formulated by using Cartesian tensor notation as follows,

$$\frac{\partial \rho}{\partial t}+\frac{\partial \rho u_i}{\partial x_i}=0 \tag{1}$$

$$\frac{\partial(\rho u_i)}{\partial t}+\frac{\partial(\rho u_i u_j)}{\partial x_j}=-\frac{\partial P}{\partial x_i}$$
$$+\frac{\partial}{\partial x_j}\left[\mu\left(\frac{\partial u_i}{\partial x_j}+\frac{\partial u_j}{\partial x_i}\right)\right] \tag{2}$$

where ρ is fluid density, u_i are the instantaneous velocity components $(i=1,2,3)$, P is the instantaneous pressure and μ dynamic viscosity of fluid. Time-averaged governing equations are obtained as Reynolds−Averaged Navier-Stokes equations (or RANS equations) when velocity and pressure terms are written as time-averaged and fluctuation terms. RANS equations can be written in Cartesian tensor form as (Ansys, 2013),

$$\frac{\partial \rho}{\partial t}+\frac{\partial \rho \overline{u}_i}{\partial x_i}=0 \tag{3}$$

$$\frac{\partial(\rho \overline{u}_i)}{\partial t}+\frac{\partial(\rho \overline{u}_i \overline{u}_j)}{\partial x_j}=-\frac{\partial \overline{P}}{\partial x_i}$$
$$+\frac{\partial}{\partial x_j}\left[\mu\left(\frac{\partial \overline{u}_i}{\partial x_j}+\frac{\partial \overline{u}_j}{\partial x_i}\right)\right]-\frac{\partial}{\partial x_j}\left(-\rho\overline{u_i' u_j'}\right) \tag{4}$$

where $\overline{u}_i$ and u_i' are the time-averaged (mean) and fluctuating velocity components. Last term $\left(-\rho\overline{u_i' u_j'}\right)$ in equation (4) represents the effects of turbulence velocity fluctuations. Various turbulence models have been developed to calculate the fluctuation terms in these equations.

2.4.2 Standard k-ε Turbulent Model

It is a semi-empirical model and has been used widely because it gives the reasonable and economical results between other two equation models for many flow phenomena in application. It includes calculation of turbulent viscosity (μ_t) and solution of two transport equations written for turbulent kinetic energy (k) and dissipation ratio (ε). These transport equations for k ve ε can be written respectively in form given in the equations (5) and (6) when effect of buoyancy forces is omitted (Ansys, 2013).

$$\frac{\partial(\rho k)}{\partial t}+\frac{\partial(\rho k u_i)}{\partial x_i}=$$
$$\frac{\partial}{\partial x_j}\left[\left(\mu+\frac{\mu_t}{\partial_k}\right)\frac{\partial_k}{\partial x_j}\right]+G_k-\rho\varepsilon \tag{5}$$

$$\frac{\partial(\rho\varepsilon)}{\partial t}+\frac{\partial(\rho\varepsilon u_i)}{\partial x_i}=\frac{\partial}{\partial x_j}\left[\left(\mu+\frac{\mu_t}{\partial_\varepsilon}\right)\frac{\partial_\varepsilon}{\partial x_j}\right]$$
$$+C_{1\varepsilon}\frac{\varepsilon}{k}G_k-C_{2\varepsilon}\rho\frac{\varepsilon^2}{k} \tag{6}$$

In these equations; k turbulence kinetic energy, μ_t turbulent (or eddy) viscosity, σ_k turbulent Prandtl number for k, G_k turbulent kinetic energy production, ε turbulent dissipation ratio, σ_ε turbulent Prandtl number for ε constants of turbulent model. The turbulent viscosity, μ_t, is given in the equation (7);

$$\mu_t=\rho C_\mu\frac{k^2}{\varepsilon} \tag{7}$$

$C_{1\varepsilon}, C_{2\varepsilon}, C_\mu, \sigma_k$ and σ_ε are the turbulent model constants. Constants of standard $k-\varepsilon$ turbulent model can be given as follows (Ansys, 2013),

$C_{1\varepsilon}=1.44, C_{2\varepsilon}=1.92, C_\mu=0.09, \sigma_k=1.0,$
$\sigma_\varepsilon=1.3$

3. FINDINGS AND DISCUSSION

In this study, pressure loss and airflow for different average velocities in a chamber with perforated V-profile diffuser designed for AHUs have been investigated numerically and experimentally. After CAD model of chamber with perforated V-profile diffuser had been created, Ansys-Fluent 14.5 Software were used for CFD analysis. CFD analysis were performed using appropriate element or mesh size and turbulence model. Three different turbulent models such as standard $k-\varepsilon$ model, realizable $k-\varepsilon$ model and $k-\omega$ model had been tried by three different element sizes to obtain better results closer to experimental results. The effect of size of volume element generated for models on the numerical results should be considered. Three different element sizes for three airflow velocities had been tried using turbulent models. In performed CFD analysis, better numerical results close to experimental results were obtained with an element size of 0.013 m (3.8×10^6 mesh number) in case of using standard $k-\varepsilon$ model as shown in Fig. 6. and Table 2.

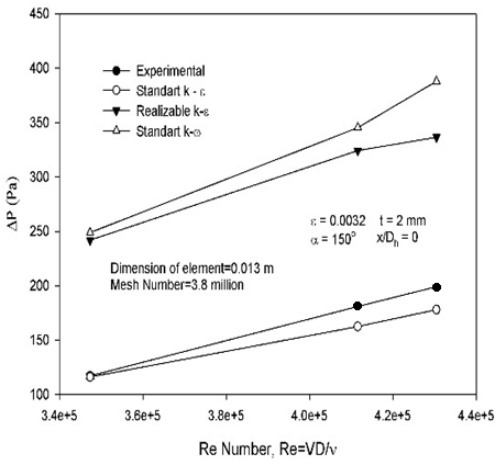

Fig. 6. Comparison of experiment data and different turbulence models for static pressure loss in the chamber.

Table 2 Element size and number of cells

V (m/s)	Element Size (m)	Number of cells (million)	ΔP (Pa) (Experimental)	ΔP (Pa) (Standard k-ε)
9.2	0.012	4.8	117	114.769
	0.013	3.8	117	116.111
	0.014	3	117	101.475
10.9	0.012	4.8	181	160.278
	0.013	3.8	181	162.622
	0.014	3	181	142.604
11.4	0.012	4.8	199	174.998
	0.013	3.8	199	177.984
	0.014	3	199	156.156

3.1 Experimental Results

Static pressures at two points shown in Fig. 4 and cross-sectional average airflow velocities at the exit of central air handling unit (AHU) given in Fig. 3 were measured. As expected, pressure drops also increases when average airflow velocity and Reynolds number increases as shown in Table 3. Reynolds numbers based averaged airflow velocity and hydraulic diameter of cross-sectional flow area of fan outlet were also given in Table 3. The kinematic viscosity of air is taken to be $\nu = 15.89 \times 10^{-6}$ m^2/s at temperature of 300 K and standard atmospheric pressure of 100 kPa.

Table 3 Experimental static pressure values.

V	Re_{D_h}	P_1	P_2	$\Delta P = P_1 - P_2$
(m/s)	-	(Pa)	(Pa)	(Pa)
9.2	3.47×10^5	603	486	117
10.9	4.11×10^5	873	692	181
11.4	4.30×10^5	944	745	199

3.2 Analysis of Numerical Results

Numerical results were obtained by using standard $k-\varepsilon$ model with an element size of 0.013 m to give better compliance with experimental results. Standard $k-\varepsilon$ model is one of the most commonly used methods in CFD analysis.

3.2.1 Effect of Dimensionless Entry Length of Diffuser

The effects of dimensionless entry length of diffuser (Fig. 2c) on static pressure loss between entry and exit sections of chamber have been investigated numerically for constant values such as apex angle of $\alpha = 150^o$, plate thickness of $t = 2$ mm and surface roughness of $R = 0.0032$ mm and the results obtained were shown in Fig. 7a. x / D_h shows the dimensionless entry length of diffuser, where is distance to diffuser from fan exit section and D_h is hydraulic diameter of fan at the exit section. Static pressure loss decreases when x / D_h increases. If entry length of diffuser increases airflow jet will diffuse by diverging before impingement to diffuser. As a result of entry static pressure to diffuser decreases, a reducing in the static pressure difference in the chamber will result.

3.2.2 Effect of Plate Thickness of Diffuser

The effects of plate thickness of diffuser on static pressure loss between entry and exit sections of chamber have been investigated numerically for constant values such as apex angle of diffuser of $\alpha = 150^o$, dimensionless entry length of diffuser of $(x / D_h = 0)$ and surface roughness of $R = 0.0032$ mm and the results obtained were shown in Fig. 7b. It was determined that static pressure loss increases in a significant manner in case that plate thickness of diffuser was changed from 2 mm to

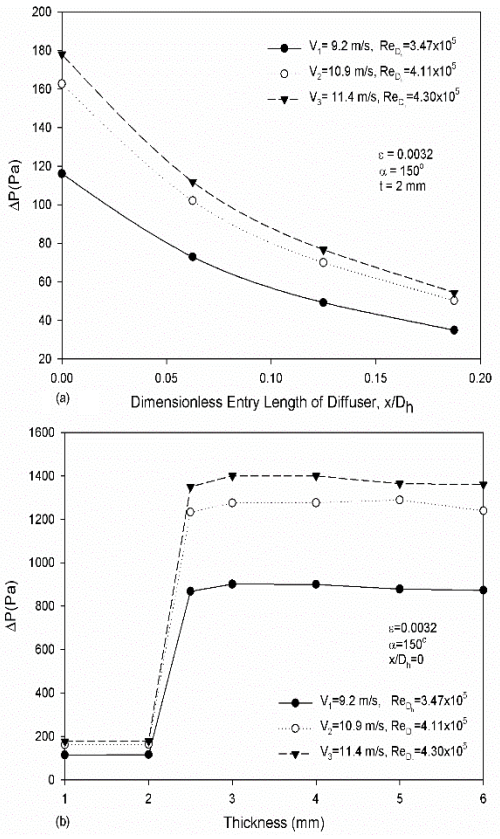

Fig. 7. (a) The effect of dimensionless entry length of diffuser (x / D_h) on the static pressure loss in the chamber. (b) The effect on static pressure loss in the chamber of plate thickness of diffuser.

2.5 mm and outside these thickness interval static pressure loss in intervals of 1-2 mm and 3-6 mm of plate thickness for all of average airflow velocities of 9.2 m/s, 10.9 m/s and 11.4 m/s. Plate thickness of 2 mm for diffuser becomes a critic length.

3.2.3 Effect of Surface Roughness of Diffuser Plate

The effects of surface roughness on static pressure loss between entry and exit sections of chamber have been investigated numerically for constant values such as apex angle of diffuser of $\alpha = 150^o$, dimensionless entry length of diffuser of $(x / D_h = 0)$ and plate thickness of diffuser of 2 mm and the results obtained were shown in Fig. 8a. The effect of surface roughness (material of diffuser plate) on static pressure loss is very low as observed Fig. 8a. Although effect of surface roughness is more important on static pressure loss, it is not observed any effect for this study because perforated plate thickness are small and Reynolds number of airflow in holes on the plate is high enough. Chamber with perforated V-plate diffuser behaves as bluff body for airflow, therefore total drag force consists of pressure (form) drag and friction drag is sufficiently very low.

3.2.4 Effect of Apex Angle of Diffuser

The effects of apex angle of diffuser on static pressure loss between entry and exit sections of chamber have been investigated numerically for constant values such as surface roughness $(R = 0.0032 \text{ mm})$, dimensionless entry length of diffuser of $(x / D_h = 0)$ and plate thickness of diffuser of 2 mm and the results obtained were shown in Fig. 8b. If apex angle of diffuser increases, drag force of perforated V-plate diffuser will also increase therefore static pressure loss will increase.

3.2.5. Effect of Hole Geometry

Static pressure losses for circular, square and equilateral triangle holes by CFD analyses in Ansys-Fluent Software were given Fig. 8c. CFD analyses have been carried out in six apex angles of diffuser by holding the porosity constant. Static pressure losses increase due to the fact that increasing form (pressure) drag when apex angle of diffuser increases for all hole geometries. The smallest pressure loss has been observed in the smallest apex angle of diffuser of 60^o because of decreasing form (pressure) drag. When pressure loss is investigated according to hole geometry, it is seen that pressure loss in circular hole is minimum for the smallest apex angle of diffuser of 60^o. In addition, pressure losses for square hole have had smaller values for the other apex angles of diffuser such as $80^o, 100^o, 120^o$ and 140^o. For high apex angles of diffuser, differences in pressure losses between square hole and the others are clearer. Cross-sectional static pressure and velocity distributions, which was 5 cm away from the downstream edge of the perforated V-profile

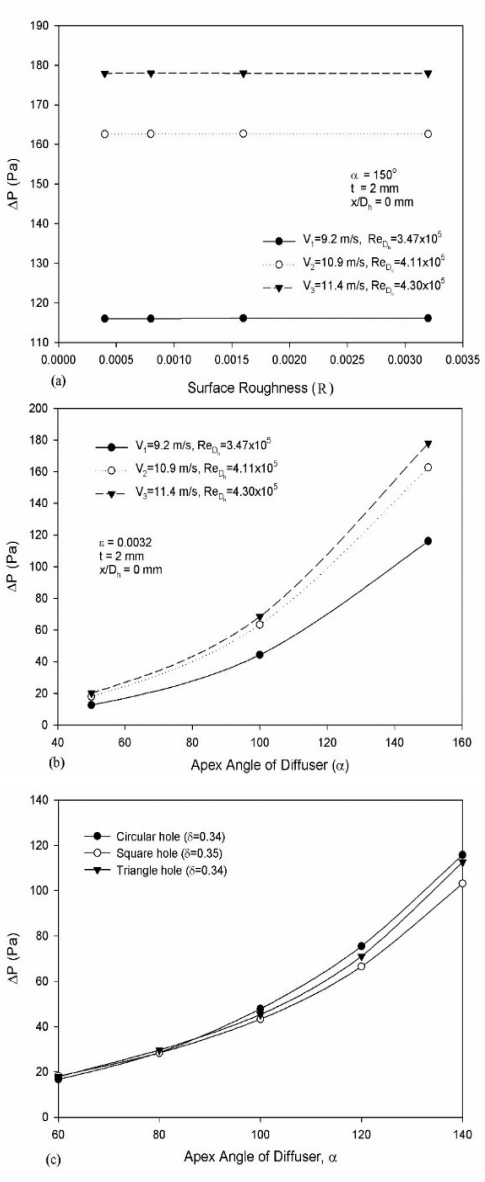

Fig. 8. (a) The effect on static pressure loss of surface roughness. (b) The effect on static pressure loss of apex angle of diffuser. (c) Comparison of static pressure losses in different apex angles of diffuser at constant porosity for circular, square and equilateral triangle holes.

diffuser with apex angle of $\alpha = 140^o$ having circular, square and equilateral triangle holes were shown in Figs 9, 10 and 11, respectively. It is observed that diffuser with square hole has more uniform pressure distribution when compared to other hole patterns. Also, a more uniform velocity distribution occurred in the middle part of the chamber with diffuser having square and equilateral triangle holes according to diffuser with circular hole.

Flow analyses for different apex angles of diffuser having square holes were carried out and it was observed that static pressure and velocity distributions on the cross section, which was 5 cm away from the downstream edge of the perforated

V-profile diffuser with apex angle of $\alpha = 140^o$ having square holes at constant porosity of $\delta = 0.35$ had a more uniform distribution according to the other apex angles of $60^o, 80^o, 100^o$ and 120^o. Turbulent pressure fluctuations in the wake region of diffuser increases as apex angle of diffuser increases and it takes the maximum value for the largest apex angle of diffuser. Velocity distribution for selecting $60^o, 100^o$ and 140^o apex angles were shown on Fig.12. It is observed that the velocity distribution in low apex angles of diffuser is very low in the middle of chamber and higher in the sides of chamber when velocity distribution examines. The velocity values in the middle of chamber becomes higher and it takes the maximum value for the largest apex angle of diffuser. As seen on Fig. 12(c), a uniform velocity distribution at the middle of chamber was obtained.

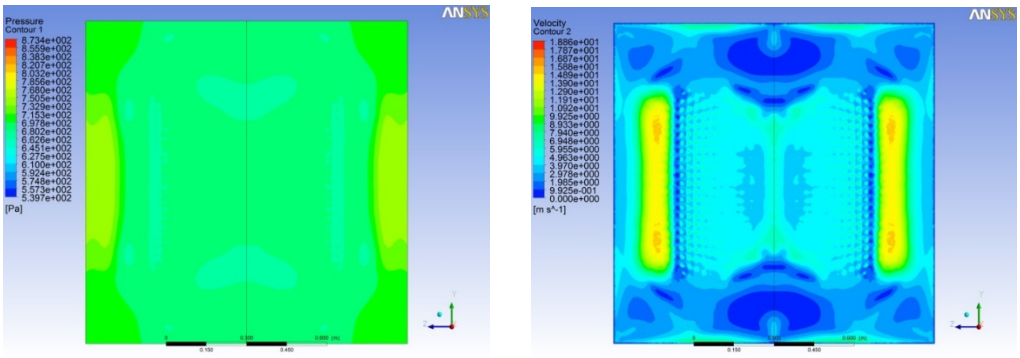

(a) (b)

Fig. 9. Cross-sectional (a) static pressure, (b) velocity distributions in the chamber with perforated V-profile diffuser with apex angle of $\alpha = 140^o$ having circular holes

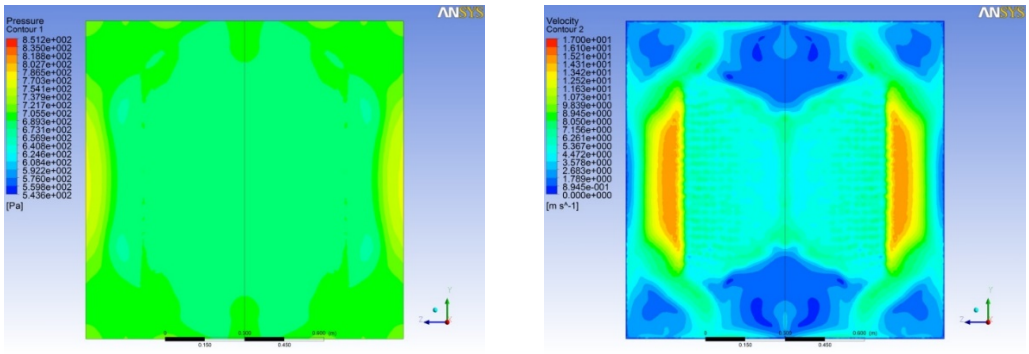

(b) (b)

Fig. 10. Cross-sectional (a) static pressure, (b) velocity distributions in the chamber with perforated V-profile diffuser with apex angle of $\alpha = 140^o$ having square holes.

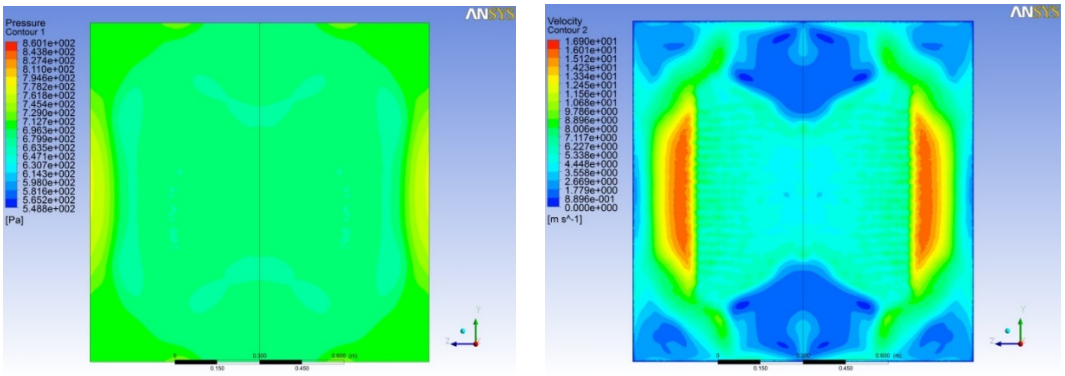

(a) (b)

Fig. 11. Cross-sectional (a) static pressure, (b) velocity distributions in the chamber with perforated V-profile diffuser with apex angle of $\alpha = 140^o$ having equilateral triangle holes.

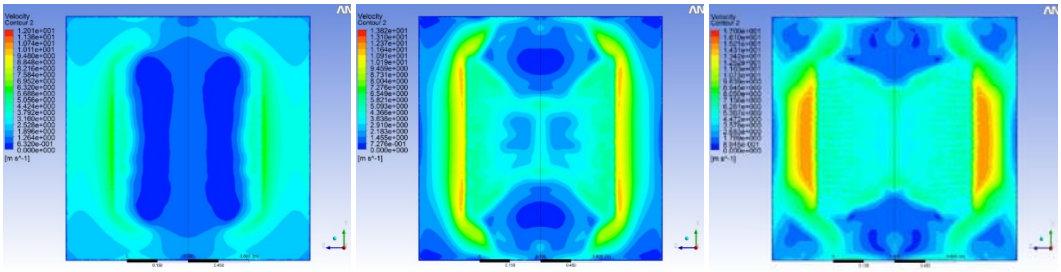

Fig. 12. Cross-sectional velocity distributions in the chamber with perforated V-profile diffuser with square holes at different apex angles

3.2.6. Effect of Porosity

The effect of porosity of diffuser plate on cross-sectional static pressure in the chamber with perforated V-profile diffuser having square holes has been investigated and the results are given in Fig. 13 due to perforated V-profile diffuser having square holes with porosity of $\delta = 0.55$ gives better results. In case of increase of porosity for all of apex angles of diffuser, decreasing in pressure losses will results in. Pressure losses for porosity of $\delta = 0.55$ at every apex angle of diffuser is minimum.

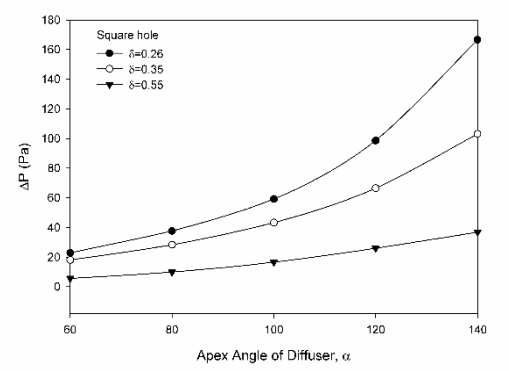

Fig. 13. Comparison of static pressure losses for different porosity values in diffusers having square holes

pressure and velocity distributions in the cross section, which was 5 cm away from the downstream edge of the perforated V-profile diffuser having square holes has been investigated and it was observed that cross-sectional static pressure and velocity distributions on the cross section of the chamber with perforated V-profile diffuser with apex angle of $\alpha = 140^o$ having square holes at constant porosity of $\delta = 0.55$ had more uniform.

3.2.7. Effect of Hole Pattern Array

The effects of square-array or staggered-array of hole pattern on variations of static pressure and velocity distributions on the exit cross section of the chamber with perforated V-profile diffuser having square holes have been investigated and the results are given in Fig. 14. It is observed that turbulent static pressure and velocity fluctuations are clearer for staggered-array although static pressure losses is approximately in the same order for each one. It is seen that pressure loss in square-array pattern is smaller than the staggered-array pattern for all apex angles of diffuser (except 60^o).

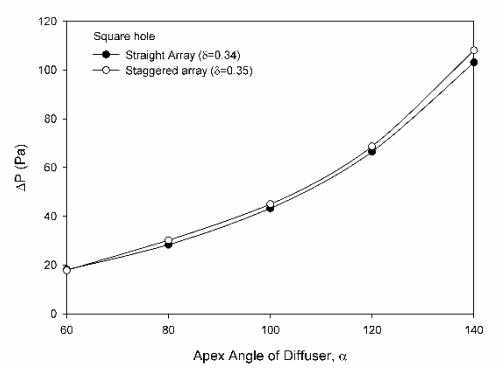

Fig. 14. Comparison of static pressure losses for different apex angles of diffuser having square holes with square-array and staggered-array pattern.

4. CONCLUSIONS

Airflow in chamber with perforated V-profile diffuser for Reynolds numbers of 3.47×10^5, 4.11×10^5 and 4.30×10^5, average airflow velocities of 9.2 m/s, 10.9 m/s and 11.4 m/s has been investigated numerically and experimentally. The following results for the effects on the velocity distribution on the exit of chamber and on the static pressure loss between entry and exit sections of chamber have been obtained depending on dimensionless entry length, apex angle, plate thickness, plate porosity, surface roughness of the diffuser and hole geometry and also array pattern on the diffuser;

– If apex angle of diffuser increases, drag force on the perforated V-plate diffuser will also increase therefore static pressure loss will increase.

– Although surface roughness on static pressure loss in many practical applications has an important effect, it is not observed any no effect for this study because perforated plate thickness are small and Reynolds number of airflow in holes on the plate is high enough. Chamber with perforated V-plate

diffuser behaves as bluff body for airflow, therefore total drag force consists of pressure (form) drag and friction drag is sufficiently very low.

- It was determined that static pressure loss increases in a significant manner in case that plate thickness of diffuser was changed from 2 mm to 2.5 mm and outside of these thickness interval static pressure loss was not change significantly for all of average airflow velocities of 9.2 m/s, 10.9 m/s and 11.4 m/s, and all of corresponding Reynolds numbers Reynolds numbers, $\mathrm{Re}_{D_h} = VD_h / \nu = 3.47 \times 10^5$, 4.11×10^5 and 4.30×10^5. Plate thickness of 2 mm for diffuser becomes a critic length.

- Static pressure loss in the chamber decreases when dimensionless entry length of diffuser x/D_h increases.

- Static pressure loss in the chamber with perforated V-profile diffuser also increases as average airflow velocity and Reynolds number increases as expected.

- In all of apex angles of diffuser (except 60o) analyzed, pressure losses in the chamber with perforated V-profile diffuser having square holes are smaller and airflow diffusion to the chamber after diffuser is more homogenous according to circular and equilateral triangle holes.

- Pressure loss decreases as porosity in the chamber with perforated V-profile diffuser having square holes increases.

- It is observed that square-array of hole pattern gives better result according to staggered-array of hole pattern although static pressure losses is approximately in the same order for each array of hole patterns in the chamber with perforated V-profile diffuser having square holes.

If an appropriate diffuser geometry and location in chamber for the AHU is selected, it is obvious that operating performance of the related following HVAC equipment such as heating/cooling coils, silencer (sound attenuator), filter or heat recovery elements will improve because of providing a uniform air diffusion from fan outlet to following chamber, internal pressure losses in AHUs will reduce, the operating or energy cost and therefore life cycle cost of the unit will also be decreased as a result of an energy efficient system design. If it is considered that electric energy has been produced from thermal power plants, which have largely used fossil fuels, the results of this study will also contribute indirectly positive environmental effects.

ACKNOWLEDGEMENTS

This study was supported by Turkish Scientific and Technological Research Council of Turkey (Project No: 114M748) and by Scientific Research Foundation of Inonu University (Project No: 2015/30).

REFERENCES

Anson, M. and L. Zhang (1995, July). On-site Abanto J., Barrero D., Reggio M. and Ozell B. (2004). Airflow modelling in a computer room. *Building and Environment* 39(12)**,** 1393-1402.

ANSYS, Fluent Theory Guide, Release 15.0, Canonsburg, 2013.

Bayazit, Y., E. M. Sparrow, D. Daniel and D. D. Joseph (2014). Perforated plates for fluid management: Plate geometry effects and flow regimes. *International Journal of Thermal Sciences* 85, 104–111.

Bayramgil, V., S. Bayrak, M. A. Yükselen and M. Z. Erim (1998, September). Experimental investigation of a diffuser for cooling and air conditioning system. *21st Congress of International Council of the Aeronautical Sciences*, Melbourne, Australia.

Bilge, M. (2010). *Air Conditioning Plants*. ISKAV Technical Book Series, Istanbul, Turkey.

Bulut, S., M. Unveren, A. Arisoy and Y. E. Boke, (2011, April). Reduction of Internal Pressure Losses in Air-Handling Units by CFD Analysis Methods. T.M.M.O.B., X. *National Plumbing Engineering Congress and Exhibition*, Izmir, Turkey.

Di Santo A., Fratino U. and Piccinni A. F. (1993). Some Considerations on The Selection Criteria of the Regulation Valves of the Large Adductors. A.I.I. Conference on *Hydraulic Machines and Equipment*, Baveno, IT Italia.

Gan, G. and Riffat S. B. (1997). Pressure loss characteristics of orifice and perforated plates. *Experimental Thermal and Fluid Science* 14(2), 160-165.

Guo, B. Y., Q. F. Hou, A. B. Yu, L. F. Li and J. Guo (2013). Numerical modelling of the gas flow through perforated plates. *Chemical Engineering Research and Design* 91(3), 403-408.

Malavasi, S., G. Messa, U. Fratino and A. Pagano (2012). On the pressure losses through perforated plates. *Flow Measurement and Instrumentation* 28, 57-66.

Noui-Mehidi, M. N., J. Wu, I. D. Sutalo and C. Grainger (2005). Velocity distribution downstream of an asymmetric wide-angle diffuser. *Experimental Thermal and Fluid Science* 29(6), 649-657.

Ozahi, E. (2015). An analysis on the pressure loss through perforated plates at moderate Reynolds numbers in turbulent flow regime. *Flow Measurement and Instrumentation* 43, 6-13.

Sahin, B. (1989). Pressure losses in an isolated perforated plate and jets emerging from the perforated plate. *International Journal of Mechanical Science* 31(1), 51-61.

Sahin, B., A. J. Ward-Smith and D. Lane (1995). The pressure drop and flow characteristics of wide-angle screened diffusers of large area ratio. *Journal of Wind Engineering and Industrial Aerodynamics* 58(1-2), 33-50.

Sahin, B. and A. J. Ward-Smith (1987). The use of perforated plates to control the flow emerging from a wide-angle diffuser, with application to electrostatic precipitator design. *Heat and Mass Transfer* 8, 124–131.

Sahin, B. and A. J. Ward-Smith (1993). The pressure distribution in and flow characteristics of wide-angle diffusers using perforated plates for flow control with application to electrostatic precipitators. *International Journal of Mechanical Science* 35(2), 117–127.

Sahin, B. and A. J. Ward-Smith (1991). Flow control by perforated plates using a blanking technique in wide-angle diffusers employed in practical electrostatic precipitator systems. *Journal of Wind Engineering and Industrial Aerodynamics* 37(3), 269–284.

Sahin, B. and A. J. Ward-Smith (1990). Effect of perforated plates on wide-angle diffuser-exit velocity profiles. *Journal of Wind Engineering and Industrial Aerodynamics* 34(2), 113–125.

SMACNA (2006). HVAC Systems Duct Design. Fourth Edition, Chapter 6.

Tacgun, E. (2016). *Klima Santrallerinde Kullanılan V Profil Delikli Difüzörlerlü Hücrenin Akış Performansının Sayısal ve Deneysel Olarak İncelenmesi*. Yüksek Lisans Tezi, İnönü Üniversitesi,Malatya, Turkey.

Tanyol, I. (2012, September). Klima Santrallerinde Enerji Tasarrufu ve CFD Analizi İle İç Dirençlerin Azaltılması. *I. Ulusal İklimlendirme Soğutma Eğitimi Sempozyumu*, Çağrılı Konuşma, Balıkesir, Turkey.

Tullis, J. P. (1989). Hydraulics of pipelines-pumps, valves, cavitation, transients New York John Wiley and Sons.